

# Deuterium-induced isotope effects on the $^{13}\text{C}$ chemical shifts of $\alpha$ -D-glucose pentaacetate

Nury Pérez-Hernández,<sup>a</sup> Celina Álvarez-Cisneros,<sup>b</sup>  
Carlos M. Cerda-García-Rojas,<sup>b</sup> Martha S. Morales-Ríos<sup>b</sup> and  
Pedro Joseph-Nathan<sup>b\*</sup>

1,2,3,4,6-Penta-O-acetyl- $\alpha$ -D-glucopyranose and the corresponding [1- $^2\text{H}$ ], [2- $^2\text{H}$ ], [3- $^2\text{H}$ ], [4- $^2\text{H}$ ], [5- $^2\text{H}$ ], and [6,6- $^2\text{H}_2$ ]-labeled compounds were prepared for measuring deuterium/hydrogen-induced effects on  $^{13}\text{C}$  chemical shift  $^n\Delta$  (DHIECS) values. A conformational analysis of the nondeuterated compound was achieved using density functional theory (DFT) molecular models that allowed calculation of several structural properties as well as Boltzmann-averaged  $^{13}\text{C}$  NMR chemical shifts by using the gauge-including atomic orbital method. It was found that the DFT-calculated C–H bond lengths correlate with  $^1\Delta$  DHIECS. Copyright © 2013 John Wiley & Sons, Ltd.

**Keywords:**  $^{13}\text{C}$  NMR; deuterium/hydrogen-induced effects;  $\alpha$ -D-glucose pentaacetate; molecular modeling; chemical shift calculations; GIAO method

## Introduction

Glucose is maybe the second central substance in human life maintenance after water. Besides its role as fuel in cells, its participation in plural biochemical functions determines the human metabolic profile in normal and pathologic states.<sup>[1]</sup> For a long time, this important monosaccharide has been subjected to many NMR analyses, from its signal assignment and  $\alpha/\beta$  configuration preference half a century ago,<sup>[2]</sup> to its recent uses as an NMR tracer signal for delineating metabolic pathways in human tissues and fluids.<sup>[3]</sup> In addition, some studies based on deuterium/hydrogen-induced effects have been used in the structure analysis,<sup>[4]</sup> hydrogen bond,<sup>[5]</sup> conformation,<sup>[6]</sup> and tautomeric equilibria<sup>[7]</sup> studies of glucose. Before the advent of 2D NMR techniques, the structure of di- and oligosaccharides was achieved by analysis of the characteristic splitting pattern of carbon signals in the glucopyranose unit with partially deuterated hydroxyl groups under slow and fast exchange conditions.<sup>[4]</sup> In another approach, deuterium-induced effects on  $^1\text{H}$  and  $^{13}\text{C}$  shifts through intra- or intermolecular hydrogen bonds have also been helpful to determine structural and conformational properties of important oligosaccharides, as cyclodextrins.<sup>[5]</sup> More recently, isotope effects have been used to establish the transition states in the  $\alpha/\beta$ -glucose interconversion,<sup>[6]</sup> as well as for determining the percentages of acyclic forms of aldohexoses in their interconversion with the cyclic forms on tautomeric equilibria.<sup>[7]</sup> Particularly for D-glucose, isotope effects on  $^{13}\text{C}$  chemical shifts induced by hydroxyl groups are very well described,<sup>[4]</sup> while isotope effects induced by deuterium atoms directly attached to the pyranose carbon atoms have been explored for the [2- $^2\text{H}$ ], [3- $^2\text{H}$ ], [5- $^2\text{H}$ ], and [6,6- $^2\text{H}_2$ ]-labeled sugar in  $\text{D}_2\text{O}$ .<sup>[8]</sup>

In this work, we describe the deuterium/hydrogen-induced effects on  $^{13}\text{C}$  chemical shift  $^n\Delta$  (DHIECS) values for [1- $^2\text{H}$ ], [2- $^2\text{H}$ ], [3- $^2\text{H}$ ], [4- $^2\text{H}$ ], [5- $^2\text{H}$ ], and [6,6- $^2\text{H}_2$ ]-D-glucose pentaacetates in  $\text{CDCl}_3$  and evaluate them in terms of structural features such as

the C–H bond lengths calculated with density functional theory (DFT) molecular models. Additionally,  $^{13}\text{C}$  NMR chemical shifts have been compared with magnetic shielding constants calculated by the gauge-including atomic orbital (GIAO)–DFT method using a correlation analysis.

## Results and Discussion

1,2,3,4,6-Penta-O-acetyl- $\alpha$ -D-glucopyranose and their corresponding [1- $^2\text{H}$ ], [2- $^2\text{H}$ ], [3- $^2\text{H}$ ], [4- $^2\text{H}$ ], [5- $^2\text{H}$ ], and [6,6- $^2\text{H}_2$ ]-labeled compounds were obtained by standard acetylation of the corresponding D-glucopyranosides. Selected  $^{13}\text{C}$  NMR shifts and one-bond CH coupling constants ( $^1J_{\text{CD}}$ ) for the  $^2\text{H}$ -labeled compounds are listed in Table 1. From these data, it can be observed that the  $^1J_{\text{CD}}$  values are approximately 24 Hz, in line with literature values for deuterated xyloses and deoxygalactoses.<sup>[8]</sup>

The  $^n\Delta$  DHIECS values were determined as the chemical shift differences of the nondeuterated and the deuterated molecules:<sup>[9]</sup>

$$^n\Delta^{13}\text{C}(\text{D}) = \delta^{13}\text{C}(\text{H}) - \delta^{13}\text{C}(\text{D}) \quad (1)$$

where  $n$  is the number of bonds between the site of deuteration and the observed carbon atom. The  $^n\Delta$  DHIECS values were

\* Correspondence to: Pedro Joseph-Nathan, Departamento de Química, Centro de Investigación y de Estudios Avanzados del Instituto Politécnico Nacional, Apartado 14-740, México, D. F., 07000 Mexico. E-mail: pjoseph@nathan.cinvestav.mx

a Programa Institucional de Biomedicina Molecular, Escuela Nacional de Medicina y Homeopatía, Instituto Politécnico Nacional, México, D. F. 07320, Mexico

b Departamento de Química, Centro de Investigación y de Estudios Avanzados del Instituto Politécnico Nacional, Apartado 14-740, México, D. F. 07000, Mexico

**Table 1.**  $\Delta$  DHIECS values (in ppb),<sup>a</sup> selected  $^{13}\text{C}$  chemical shifts (in ppm), and  $^2\text{H}$ - $^{13}\text{C}$  coupling constants (in Hz) of deuterated  $\alpha$ -D-glucose pentaacetates

Carbon	D-[1- $^2\text{H}$ ]-Glu	D-[2- $^2\text{H}$ ]-Glu	D-[3- $^2\text{H}$ ]-Glu	D-[4- $^2\text{H}$ ]-Glu	D-[5- $^2\text{H}$ ]-Glu	D-[6,6- $^2\text{H}_2$ ]-Glu
C1	$^1\Delta = -273$ 88.7, $t, J = 27$	$^2\Delta = -39$				
C2	$^2\Delta = -73$	$^1\Delta = -317$ 68.8, $t, J = 23.2$	$^2\Delta = -67$			
C3	$^3\Delta = -20$	$^2\Delta = -54$	$^1\Delta = -298$ 69.5, $t, J = 26.2$	$^2\Delta = -69$		
C4			$^2\Delta = -69$	$^1\Delta = -314$ 67.4, $t, J = 24.1$	$^2\Delta = -49$	$^3\Delta = -10$
C5	$^3\Delta = -20$			$^2\Delta = -69$	$^1\Delta = -365$ 69.3, $t, J = 24.1$	$^2\Delta = -114$
C6				$^3\Delta = -19$	$^2\Delta = -53$	$^1\Delta = -543$ 60.8, $q, J = 22.8$
C=O (2)		$^3\Delta = -3$				
C=O (3)			$^3\Delta = -10$			
C=O (4)				$^3\Delta = -9$		$^5\Delta = 5$
C=O (6)						$^3\Delta = 13$
Me (2)			$^5\Delta = -2$			
Me (3)			$^4\Delta = -2$	$^5\Delta = -3$		
Me (4)			$^5\Delta = -3$			
Me (6)				$^6\Delta = 3$		$^4\Delta = 3$

<sup>a</sup>The acetate carbons at C1 showed no measurable shifts.

measured under uniform conditions (see Experimental Section) and are also summarized in Table 1. According to the general trend,<sup>[9]</sup> the  $^{1-3}\Delta$  DHIECS values decrease when the number of bonds between the deuterium atom and the observed  $^{13}\text{C}$  atom increases, while  $^{4,5}\Delta$  DHIECS values are exceptions to this tendency. The  $^1\Delta$  DHIECS values exhibit a negative sign and are in the range of  $-273$  to  $-365$  parts per billion (ppb =  $10^{-9}$ ) for monodeuterated pentaacetates, while for the dideuterated pentaacetate, the magnitude increased almost twice, to  $-543$  ppb, keeping the direct proportionality between the shift magnitude and the number of substituted deuterium atoms.<sup>[10]</sup> The smallest  $^1\Delta$  DHIECS value was observed for [1- $^2\text{H}$ ]- $\alpha$ -D-glucose pentaacetate, an expected consequence of the strong deshielding effect of two electronegative oxygen atoms in the anomeric position. The remaining  $^1\Delta$  DHIECS in increasing order for the net value are as follows:  $-298$ ,  $-314$ ,  $-317$ , and  $-365$  ppb, for [3- $^2\text{H}$ ], [4- $^2\text{H}$ ], [2- $^2\text{H}$ ], and [5- $^2\text{H}$ ] pentaacetates, respectively.

The  $^2\Delta$  DHIECS values exhibit a negative sign and are in the range of  $-49$  to  $-114$  ppb. As expected, the largest value was observed for the dilabeled [6,6- $^2\text{H}_2$ ]- $\alpha$ -D-glucose that showed  $^1\Delta = -114$  ppb. For monodeuterated compounds, the largest  $^2\Delta$  was  $-73$  ppb at C2 of [1- $^2\text{H}$ ]-pentaacetate, while the smallest value of  $-39$  was observed for C1 of [2- $^2\text{H}$ ]-pentaacetate. Long-range  $^3\Delta$  DHIECS were observed for [1- $^2\text{H}$ ], [2- $^2\text{H}$ ], [3- $^2\text{H}$ ], [4- $^2\text{H}$ ], and [6,6- $^2\text{H}_2$ ]-glucose pentaacetates. For monolabeled glucoses, the  $^3\Delta$  isotope effects are negative and span the range  $-3$  to  $-20$  ppb. As seen from Table 1, the  $^3\Delta$  values for the glucopyranose ring are larger,  $-20$  ppb in average, than those for the carbonyl carbons,  $-3$  to  $-10$  ppb range, in agreement with the deshielding effect of the two oxygen atoms in the carbonyl groups which affects more the deuterium shielding effect of the  $^{13}\text{C}$  chemical shift. On the contrary, in dilabeled [6,6- $^2\text{H}_2$ ]-glucose pentaacetate, the  $^3\Delta$  DHIECS magnitudes are inverted, as was mentioned before, reflecting that the additive shielding effect by two deuterium atoms is more effective than the electronegative

effect in the  $^{13}\text{C}$  signal. Also,  $^4\Delta$ ,  $^5\Delta$ , and even  $^6\Delta$  DHIECS values were observed for [3- $^2\text{H}$ ], [4- $^2\text{H}$ ], and [6,6- $^2\text{H}_2$ ]-pentaacetates. For monodeuterated sugars, the values show in general a negative sign contrary to the dilabeled compound. Thus, for [3- $^2\text{H}$ ] pentaacetate, a  $^4\Delta$  DHIECS value of  $-2$  ppb was observed at Me-3, and additionally, two  $^5\Delta$  DHIECS values at Me-2 and Me-4 with similar values, approximately  $-3$  ppb, were also found. For [4- $^2\text{H}$ ] pentaacetate, a  $^5\Delta$  DHIECS value of  $-3$  ppb was observed at Me-3, and a  $^6\Delta$  DHIECS with the same value but opposite sign (3 ppb) was found at Me-6. For [6,6- $^2\text{H}_2$ ]-pentaacetate, a  $^4\Delta$  DHIECS value of 3 ppb was observed at C=O(3) and a  $^5\Delta$  DHIECS value of 5 ppb was measured at Me-6. The positive shift for  $^3\Delta$ ,  $^4\Delta$ , and  $^5\Delta$  DHIECS values in dilabeled [6,6- $^2\text{H}_2$ ]-glucose pentaacetate could be explained by a combinatory effect arising from several geometries adopted by the  $-\text{CD}_2\text{OCOCH}_3$  group involving nonadditive and second-order terms.<sup>[11]</sup>

In order to find correlations between DHIECS and structural properties of 1,2,3,4,6-penta-*O*-acetyl- $\alpha$ -D-glucopyranose (**1**), a molecular model of this substance was obtained by means of DFT calculations. The initial structure of **1** was built using its X-ray atom coordinates. A search in the Cambridge Crystallographic Data Centre (CCDC) database showed the four deposits ZZZQPG01, ZZZRCA01, ZZZRCA, and ZZZRCA02 for **1**. The first two records provided no atom coordinates, while in the remaining two files, data were refined to  $R_1$  values of 7.3% and 4.6%, respectively. Therefore, to obtain a more precise set of atomic coordinates, we performed a single crystal X-ray analysis of **1**, which was refined to  $R_1 = 3.7\%$  (Fig. 1). These coordinates were loaded into the Spartan'04 program (Wavefunction, Irvine, CA, USA), and the molecular model was subjected to an energy minimization routine employing the molecular mechanics force field (MMFF). An exhaustive Monte Carlo search<sup>[12]</sup> afforded 31 conformations within the first 3 kcal/mol. The whole set was subjected to a DFT single-point energy calculation at the B3LYP/6-31G(d) level of theory, reducing the number of conformers to eight

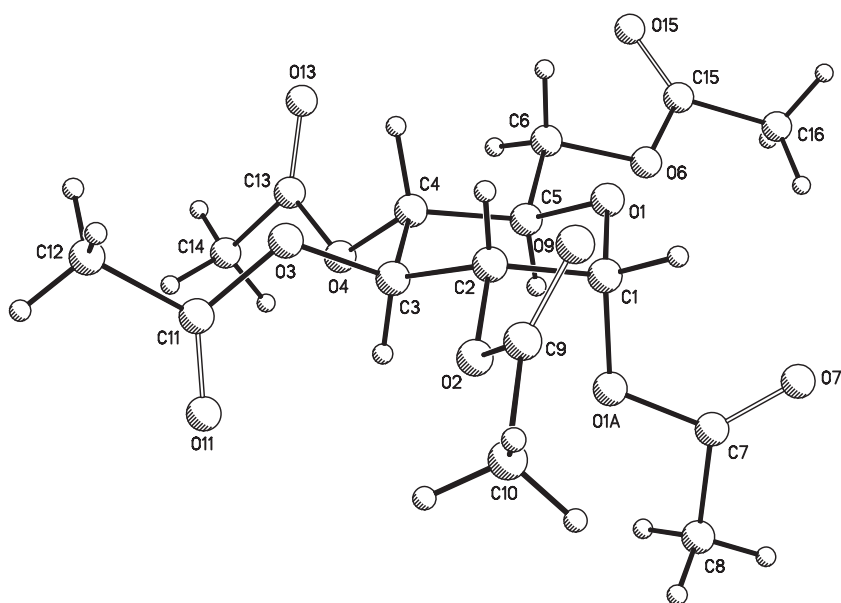


**Figure 1.** X-ray diffraction structure of 1,2,3,4,6-penta-*O*-acetyl- $\alpha$ -D-glucopyranose (**1**).

minima. Geometry optimization, vibrational frequencies, and thermochemical parameter calculations of these structures were carried out at the B3PW91/DGDZVP and the B3LYP/6-311+G(2d,p) levels of theory<sup>[13]</sup> in the presence of CHCl<sub>3</sub> using the Gaussian 03 program (Gaussian Inc., Wallingford, CT, USA). This procedure gave four main conformers (**1a–1d**) that, according to the  $\Delta G = -RT \ln K$  equation, accounted for 97.8% of the conformational population using the B3PW91/DGDZVP level of theory (Fig. 2) and for 96.4% using the B3LYP/6-311+G(2d,p) level of theory (Fig. 3). These structures essentially preserved the same spatial arrangements of the O1–C1–C2–C3–C4–C5 framework, including the ester residues at C1 to C4, but showed changes in

the rotation of the C5–C6 bond and in the orientation of the acetyl group at C6. In both levels of theory, the global minimum structure showed a *gg* conformation in the C5–C6 bond, followed by *gt* or *gg* conformational variants. The absence of any *tg* conformer was remarkable and in line with a previous experimental analysis of the rotameric distribution for the C5–C6 bond of **1**.<sup>[14]</sup> It is worth mentioning that the B3PW91/DGDZVP models reproduced more faithfully the observed *gg:gt:tg* conformational ratio.<sup>[14]</sup> In addition, the magnetic shielding tensors were calculated for the selected conformers with the GIAO method,<sup>[15]</sup> which were Boltzmann-weighted taking into account the DFT population, referenced using TMS values

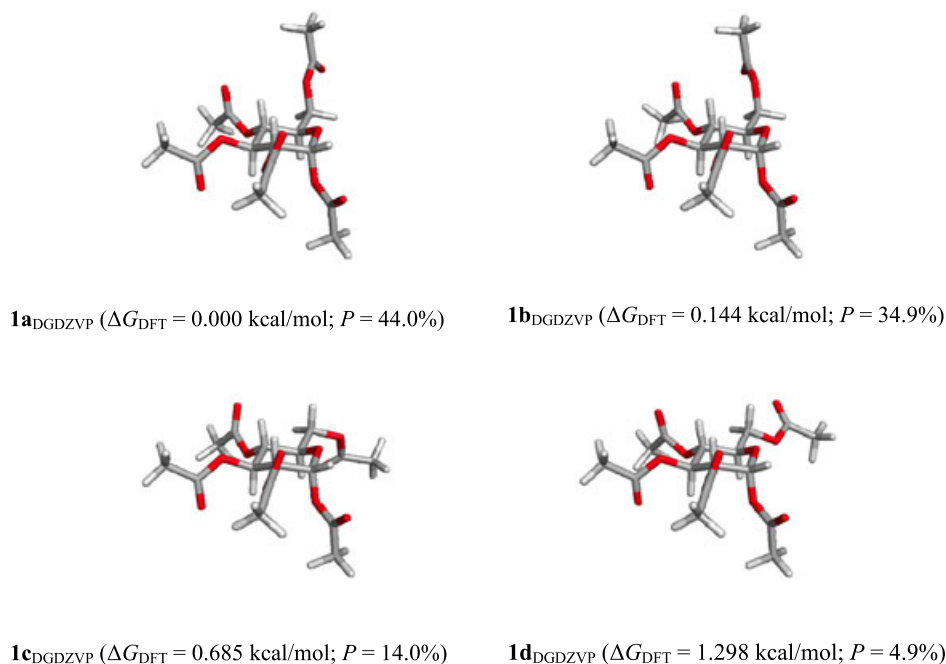


**Figure 2.** Minimum energy structures for 1,2,3,4,6-penta-*O*-acetyl- $\alpha$ -D-glucopyranose at the B3PW91/DGDZVP level of theory.

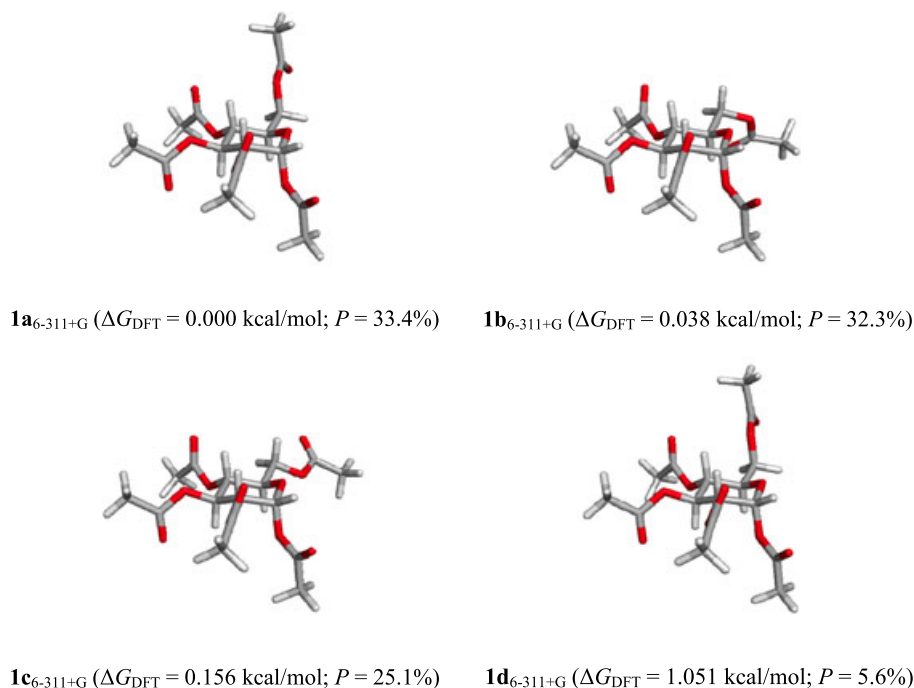


**Figure 3.** Minimum energy structures for 1,2,3,4,6-penta-*O*-acetyl- $\alpha$ -D-glucopyranose at the B3LYP/6-311+G(2d,p) level of theory.

calculated with the same basis sets, and scaled using a factor obtained by iteration for each basis set. The scaling factors ( $f$ ) were calculated to compensate for the moderately overvalued shielding tensors arising from the limitations of the DFT-GIAO methods.<sup>[16]</sup> The  $f$  values were determined by an iterative process that minimized the root-mean-square deviation between the calculated and observed chemical shifts. For the B3PW91/DGDZVP,  $f$  was 0.963, while for the B3LYP/6-311+G(2d,p) level of theory,  $f$  was 0.953. In addition, a slight correction for the TMS chemical shift

of  $\delta$  1.320 for the B3PW91/DGDZVP and of  $\delta$  1.040 for the B3LYP/6-311+G(2d,p) was applied. The calculated  $^{13}\text{C}$  NMR chemical shifts of  $\alpha$ -D-glucose pentaacetate for the two functionals/basis sets are listed in Table 2, where they can be contrasted with the experimental values.

Correlation between theoretical and experimental chemical shift values is related to the accuracy of the used molecular models, as shown in Table 2 and Fig. 4. The complete process involves geometry optimization, vibrational frequencies, and GIAO chemical shift

**Table 2.** Experimental and calculated  $^{13}\text{C}$  NMR chemical shifts (in ppm) for  $\alpha$ -D-glucose pentaacetate (**1**)

Carbon	Exp	B3PW91/DGDZVP			B3LYP/6-311+G(2d,p)		
		Calcd	Corrected <sup>a</sup>	$\Delta_{\text{exp-corr}}$	Calcd	Corrected <sup>b</sup>	$\Delta_{\text{exp-corr}}$
C1	89.0	95.5	90.7	-1.7	95.2	89.7	-0.7
C2	69.1	73.0	69.0	0.1	74.6	70.1	-1.0
C3	69.7	71.5	67.6	2.2	73.7	69.2	0.5
C4	67.8	69.3	65.4	2.3	72.5	68.1	-0.3
C5	69.7	74.8	70.7	-1.0	76.6	72.0	-2.3
C6	61.6	65.6	61.9	-0.3	67.5	63.3	-1.7
C=O (1)	168.7	176.8	168.9	-0.2	178.0	168.6	0.1
C=O (2)	169.6	178.0	170.0	-0.4	178.7	169.3	0.3
C=O (3)	170.1	177.5	169.6	0.5	178.6	169.2	0.9
C=O (4)	169.3	177.3	169.3	0.0	178.5	169.1	0.2
C=O (6)	170.5	179.0	171.0	-0.4	179.7	170.3	0.2
OMe (1)	20.8	23.1	21.0	-0.2	22.2	20.1	0.7
OMe (2)	20.4	22.8	20.6	-0.3	21.8	19.8	0.6
OMe (3)	20.5	23.2	21.1	-0.6	22.1	20.1	0.4
OMe (4)	20.6	23.2	21.0	-0.4	22.1	20.0	0.6
OMe (6)	20.6	23.2	21.1	-0.5	21.9	19.9	0.7

<sup>a</sup> $\delta_{\text{corrected}} = 0.963 (\delta_{\text{calculated}} - 1.320)$ , factors obtained by iteration, RMS = 0.995 ppm.

<sup>b</sup> $\delta_{\text{corrected}} = 0.953 (\delta_{\text{calculated}} - 1.040)$ , factors obtained by iteration, RMS = 0.909 ppm.

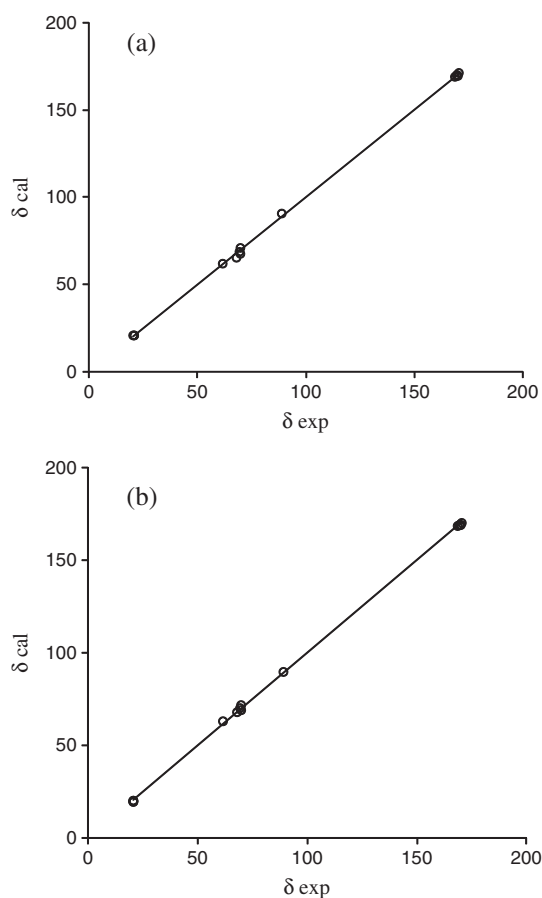


**Figure 4.** Correlation of the experimental and DFT calculated  $^{13}\text{C}$  NMR chemical shifts for 1,2,3,4,6-penta-*O*-acetyl- $\alpha$ -D-glucopyranose (a) using GIAO-DFT B3PW91/DGDZVP PCM shielding constants ( $\delta_{\text{cal}} = 0.9997 \delta_{\text{exp}} + 0.0729$ ,  $R^2 = 0.9997$ ); (b) using GIAO-DFT B3LYP/6-311+G(2d,p) PCM shielding constants ( $\delta_{\text{cal}} = 0.9992 \delta_{\text{exp}} + 0.1138$ ,  $R^2 = 0.9998$ ).

calculations, which for the B3PW91/DGDZVP functional/basis set required approximately 24 h per conformer, while for the B3LYP/6-311+G(2d,p) functional/basis set required approximately 96 h per conformer. Given that calculations for eight conformers per model were required, the data for both levels of theory are included in Table 2, to provide diagnostic information to compare accuracy and computer costs.

It has been reviewed that isotope effects arise from changes in the average bond distance of the X–H bond upon deuteration,<sup>[10]</sup> and it has been noticed that the magnitude of isotope effects increases with increasing bond length,<sup>[17]</sup> as observed for axial versus equatorial C–H bonds in cyclohexane.<sup>[18]</sup> Accordingly, in

the present study, it was found that the C–H bond lengths for C1–H to C5–H, calculated at the DFT B3PW91/DGDZVP and B3LYP/6-311+G(2d,p) levels of theory (Table 3) using  $\text{CHCl}_3$  as implicit solvent, closely correlate with the magnitude of  $^1\Delta$  DHIECS (Fig. 5), suggesting that this relationship can be originated by the same phenomenon that involves bond distance variations.<sup>[17]</sup> Bond lengths and  $^1\Delta$  DHIECS values for the C6–H<sub>2</sub> moiety were not included in the plot because they follow a more complex pattern arising from differences in the substitution, the combinatory effect of the previously mentioned changing geometries adopted by the  $-\text{CD}_2\text{OCOCH}_3$  group, and the influence of the two deuterium atoms.<sup>[17]</sup>

Assignment of the  $^{13}\text{C}$  NMR acetate signals was done using HMBC spectra. Three-bond cross-peaks between the  $^1\text{H}$  signals of the pyranose ring and the  $^{13}\text{C}$  carbonyl signals were observed as follows: H1 at  $\delta$  6.34 with the signal at  $\delta$  168.7, H2 at  $\delta$  5.10 with the signal at  $\delta$  169.6, H3 at  $\delta$  5.48 with the signal at  $\delta$  170.1, H4 at  $\delta$  5.15 with that of  $\delta$  169.3, and the  $\text{CH}_2$ 6 at  $\delta$  4.27 and 4.10 with the signal at  $\delta$  170.5. Additionally, the methyl group  $^1\text{H}$  signals were assigned using their correlations with the already assigned carbonyl groups as follows: CO1 with the signal at  $\delta$  2.18, CO2 with the signal at  $\delta$  2.02, CO3 with the signal at  $\delta$  2.03, CO4 with the signal at  $\delta$  2.04, and CO6 with the signal at  $\delta$  2.10. The assignment of the corresponding  $^{13}\text{C}$  signals for the methyl groups was made from their HSQC correlations.

## Experimental

### General experimental procedures

[1- $^2\text{H}$ ], [2- $^2\text{H}$ ], and [6,6- $^2\text{H}_2$ ]-D-glucose were obtained from Sigma Aldrich, while [3- $^2\text{H}$ ], [4- $^2\text{H}$ ], and [5- $^2\text{H}$ ]-D-glucose were obtained from Omicron Biochemicals, Inc. Sugars were used without further purification. The melting point was determined on a Fisher–Johns melting point apparatus and is uncorrected.

### Acetylation of D-glucoses

A solution of D-glucose or of  $^2\text{H}$ -labeled D-glucoses (30 mg, 0.08 mmol) in pyridine (1.5 ml) was cooled in an ice bath, and acetic anhydride (1 ml) was added under stirring. The reaction mixture was kept for 72 h at room temperature. Then, in an ice bath,  $\text{H}_2\text{O}$  (1.5 ml) was added, and the reaction mixture was extracted with AcOEt ( $3 \times 20$  ml). The combined organic extract was washed with 10% HCl ( $3 \times 20$  ml), with  $\text{H}_2\text{O}$  (20 ml), with a 5% solution of  $\text{NaHCO}_3$  (20 ml), and with  $\text{H}_2\text{O}$  again, dried over anhydrous  $\text{Na}_2\text{SO}_4$ , filtered, and evaporated under vacuum. The corresponding acetylated glucoses (62 mg, 96% in average) were

**Table 3.**  $^1\Delta$  DHIECS values (in ppb) for deuterated  $\alpha$ -D-glucose pentaacetates and DFT-calculated C–H bond lengths (in Å) of 1,2,3,4,6-penta-*O*-acetyl- $\alpha$ -D-glucopyranose (**1**) at the B3PW91/DGDZVP and the B3LYP/6-311+G(2d,p) levels of theory

$^2\text{H}$ position	$^1\Delta$ DHIECS	Bond	B3PW91/DGDZVP C–H bond length <sup>a</sup>	B3LYP/6-311+G(2d,p) C–H bond length <sup>a</sup>
C1	–272.5	C1–H	1.091	1.088
C2	–316.8	C2–H	1.093	1.091
C3	–297.6	C3–H	1.092	1.089
C4	–314.4	C4–H	1.092	1.091
C5	–364.6	C5–H	1.097	1.094

<sup>a</sup>Boltzmann-averaged values.

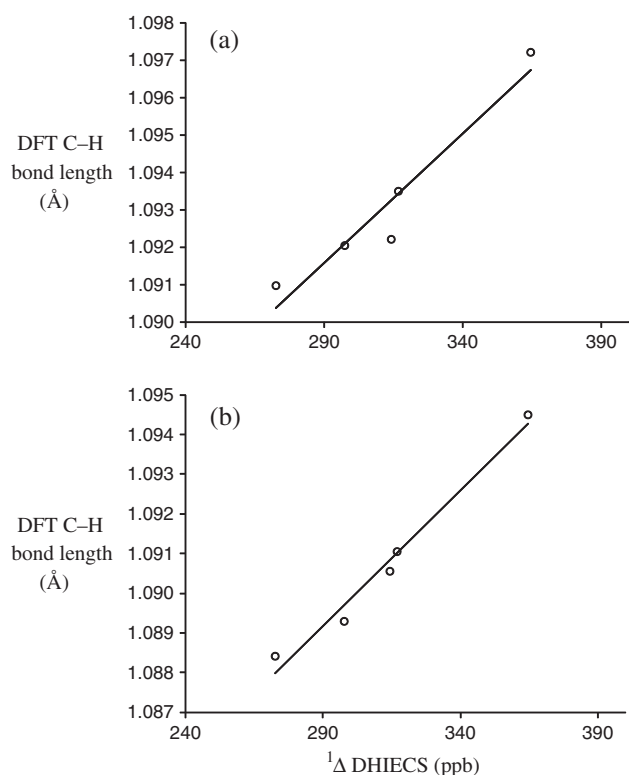


**Figure 5.** Correlation between the DFT-calculated C–H bond lengths of 1,2,3,4,6-penta-*O*-acetyl- $\alpha$ -D-glucopyranose and the magnitude of  $^1\Delta$  DHIECS at (a) the B3PW91/DGDZVP level of theory (DFT C–H bond length =  $7 \times 10^{-5} \Delta$  DHIECS + 1.072,  $R^2 = 0.926$ ) and (b) the B3LYP/6-311+G(2d,p) level of theory (DFT C–H bond length =  $7 \times 10^{-5} \Delta$  DHIECS + 1.069,  $R^2 = 0.978$ ).

obtained as a 4:1 mixture of  $\alpha/\beta$  isomers. The  $\alpha$ -isomers were purified by successive recrystallizations using THF-hexanes (5:1) to provide colorless plates mp 100–101 °C.

### NMR experiments

NMR measurements were carried out on a Varian Mercury spectrometer at 75.4 MHz for  $^{13}\text{C}$  using a 5-mm probe from  $\text{CDCl}_3$  solutions. Coupling constant values are given in Hz, and chemical shifts are reported in ppm from internal TMS registered with a magnet homogeneity better than  $W_{1/2} = 0.20$  Hz measured at the TMS signal. For the DHIECS measurements, 0.83 M  $\text{CDCl}_3$  solutions of the unlabeled/labeled glucoses in a 7:3 ratio were degassed by bubbling argon, and measurements were performed at 300 ( $\pm 1$ ) K. The  $^1\text{H}$  interactions were eliminated using the low-energy Waltz-16 decoupling pulse technique.<sup>[19]</sup> For data acquisition, the pulse width was set to 20.5° (5  $\mu\text{s}$ ), the recycling time was set to 5 s, and at least 26 544 data points were acquired. The FID data were zero-filled to 128 k data points prior to Fourier transformation providing digital resolution of at least 0.081 Hz per point (1.1 ppb). The NMR data were processed on a SUN ULTRA 60 workstation using the SOLARIS 9 platform and VNMR 6.1c software.

### Single crystal X-ray diffraction analysis of 1

A crystal measuring 0.24  $\times$  0.14  $\times$  0.06 mm, obtained by crystallization from THF-hexane, was mounted on an Enraf-Nonius CAD4 diffractometer equipped with  $\text{CuK}\alpha$  radiation ( $\lambda = 1.54184$  Å). The data

were collected at 293(2) K in the  $\omega$ -2 $\theta$  scan mode. Unit cell refinements using 25 machine-centered reflections were done using the CAD4 Express v2.0 software. Crystal data were  $\text{C}_{16}\text{H}_{22}\text{O}_{11}$ ,  $M = 390.34$ , orthorhombic, space group  $P2_12_12_1$ ,  $a = 5.584(2)$  Å,  $b = 14.713(1)$  Å,  $c = 23.958(2)$  Å,  $V = 1968.4(6)$  Å<sup>3</sup>,  $Z = 4$ ,  $\rho = 1.32$  mg/mm<sup>3</sup>,  $\mu(\text{CuK}\alpha) = 0.975/\text{mm}$ , total reflections = 1634, unique reflections 1535 ( $R_{\text{int}} = 0.01\%$ ), observed reflections 1352, final  $R$  indices [ $I > 2\sigma(I)$ ]  $R_1 = 3.7\%$ ,  $wR_2 = 10.0\%$ . The structure was solved by direct methods using the SHELXS-97 program included in the WinGX v1.70.01 crystallographic software package. For the structural refinement, the nonhydrogen atoms were treated anisotropically, and the hydrogen atoms, included in the structure factor calculation, were refined isotropically. Crystallographic data (excluding structure factors) have been deposited at the CCDC. The CCDC deposition number is 911297. Copies of the data can be obtained free of charge on application to CCDC, 12 Union Road, Cambridge CB2 1EZ, UK (fax: +44-(0)1223-336033; e-mail: deposit@ccdc.cam.ac.uk).

### Computational analysis

The molecular model of 1,2,3,4,6-penta-*O*-acetyl- $\alpha$ -D-glucopyranose was constructed using the X-ray atom coordinates and subjected to a full minimization routine employing molecular mechanics (MMFF), in the Spartan'04W package (Wavefunction, Irvine, CA, USA). The conformational search was made with the Monte Carlo protocol,<sup>[11]</sup> obtaining a total of 31 conformers in the first 3 kcal/mol. These structures were then submitted to geometry optimization by DFT calculations at the B3LYP/6-31G (d) level of theory to provide eight minimum energy structures, which were reoptimized at the B3PW91/DGDZVP and B3LYP/6-311+G(2d,p) levels of theory in the presence of  $\text{CHCl}_3$  perturbation using the polarizable continuum model as implemented in the Gaussian 03W program (Gaussian Inc., Wallingford, CT, USA), providing four representative minimum energy conformers (**1a–1d**) for each level. The geometries of these four DFT conformers were then used for estimate the NMR shielding tensors through the GIAO method.<sup>[14]</sup> The calculated NMR shielding tensors were converted into chemical shifts ( $\delta$ ), considering the isotropic values of the shielding tensors of the  $^{13}\text{C}$  atom in TMS, calculated at the same levels of theory as  $\delta$  184.63 for B3PW91/DGDZVP and  $\delta$  183.61 for B3LYP/6-311+G(2d,p).

### Acknowledgements

Partial financial support from Conacyt-México, grant 61122, is acknowledged.

### References

- (1) (a) L. I. Malinova, T. P. Denisova, in *Handbook of Optical Sensing of Glucose in Biological Fluids and Tissues* (Eds. J. G. Webster, E. R. Ritenour, S. Tabakov, K.-H. Ng), Taylor & Francis Group, Florida, **2009**, pp. 1–40. (b) D. H. Wasserman, *Am. J. Physiol. Endocrinol. Metab.* **2009**, 296, E11.
- (2) (a) R. U. Lemieux, R. K. Kullnig, H. J. Bernstein, W. G. Schneider, *J. Am. Chem. Soc.* **1957**, 79, 1005; (b) R. U. Lemieux, R. K. Kullnig, H. J. Bernstein, W. G. Schneider, *J. Am. Chem. Soc.* **1958**, 80, 6098; (c) B. Casu, M. Reggiani, G. G. Gallo, A. Vigevari, *Tetrahedron Lett.* **1964**, 5, 2839; (d) B. Casu, M. Reggiani, G. G. Gallo, A. Vigevari, *Tetrahedron Lett.* **1965**, 6, 2253; (e) R. U. Lemieux, J. D. Stevens, *Can. J. Chem.* **1966**, 44, 249; (f) A. S. Perlin, B. Casu, *Tetrahedron Lett.* **1969**, 34, 2921.
- (3) (a) T. W. M. Fan, A. N. Lane, *J. Biomol. NMR*, **2011**, 49, 267; (b) J. L. Sébédio, E. Pujos-Guillot, M. Ferrara, *Curr. Opin. Clin. Nutr. Metab. Care* **2009**, 12, 412; (c) M. A. García-Espinosa, T. B. Rodrigues, A. Sierra, M. Benito, C. Fonseca, H. L. Gray, B. L. Bartnik, M. L. García-Martín, P. Ballesteros, S. Cerdán, *Neurochem. Int.* **2004**, 45, 297; (d) M. Roden, K. F. Petersen, G. I. Shulman, *Recent Prog. Horm. Res.* **2001**, 56, 219.

- [4] (a) H. J. Koch, R. S. Stuart, *Carbohydr. Res.* **1977**, 59, C1; (b) D. Gagnaire, M. Vincendon, *J. Chem. Soc. Chem. Commun.* **1977**, 509; (c) D. Gagnaire, D. Mancier, M. Vincendon, *Org. Magn. Reson.* **1978**, 11, 344; (d) P. E. Pfeffer, K. M. Valentine, F. W. Parrish, *J. Am. Chem. Soc.* **1979**, 101, 1265; (e) P. E. Pfeffer, F. W. Parrish, J. Unruh, *Carbohydr. Res.* **1980**, 84, 13. (f) J. C. Christofides, D. B. Davies, *J. Am. Chem. Soc.* **1983**, 105, 5099; (g) J. Reuben, *J. Am. Chem. Soc.* **1983**, 105, 3711; (h) J. C. Christofides, D. B. Davies, *J. Chem. Soc. Chem. Commun.* **1983**, 324; (i) J. Reuben, *J. Am. Chem. Soc.* **1984**, 106, 6180; (j) J. Reuben, *J. Am. Chem. Soc.* **1985**, 107, 1747.
- [5] (a) M. St-Jacques, P. R. Sundararajan, K. J. Taylor, R. H. Marchessault, *J. Am. Chem. Soc.* **1976**, 98, 4386; (b) J. C. Christofides, D. B. Davies, *J. Chem. Soc. Chem. Commun.* **1982**, 560; (c) M. Bock, K. Lemieux, U. Raymond, *Carbohydr. Res.* **1982**, 100, 63; (d) J. J. C. Christofides, D. B. Davies, *J. Chem. Soc. Chem. Commun.* **1985**, 1533; (e) J. C. Christofides, D. B. Davies, *Magn. Reson. Chem.* **1985**, 23, 582; (f) J. C. Christofides, D. B. Davies, *J. Chem. Soc. Perkin Trans. 2* **1987**, 97; (g) S. Kitamura, H. Isudaa, J. Shimadab, T. Takadab, T. Takahac, S. Okadac, M. Mimurad, K. Kajjwarad, *Carbohydr. Res.* **1997**, 304, 303; (h) A. Gamini, R. Toffanin, E. Murano, R. Rizzo, *Carbohydr. Res.* **1997**, 304, 293; (i) C. Sandström, H. Baumann, L. Kenne, *J. Chem. Soc. Perkin Trans. 2* **1998**, 809.
- [6] (a) B. E. Lewis, N. Choytun, V. L. Schramm, A. J. Bennet, *J. Am. Chem. Soc.* **2006**, 128, 5049; (b) B. E. Lewis, V. L. Schramm, *J. Am. Chem. Soc.* **2001**, 123, 1327.
- [7] Y. Zhu, J. Zajicek, A. S. Serianni, *J. Org. Chem.* **2001**, 66, 6244.
- [8] (a) P. A. J. Gorin, *Can. J. Chem.* **1974**, 52, 458; (b) P. A. J. Gorin, M. Mazurek, *Can. J. Chem.* **1975**, 53, 1212.
- [9] (a) R. Aydin, J. R. Wesener, H. Günther, R. L. Santillan, M. E. Garibay, P. Joseph-Nathan, *J. Org. Chem.* **1984**, 49, 3845; (b) T. Dziembowska, P. E. Hansen, Z. Rozwadowski, *Prog. Nucl. Mag. Res. Sp.* **2004**, 45, 1.
- [10] P. E. Hansen, *Magn. Reson. Chem.* **2000**, 38, 1.
- [11] R. D. Wigglesworth, W. Raynes, S. Kirpekar, J. Oddershede, S. Sauer, *J. Chem. Phys.* **2000**, 112, 736.
- [12] J. J. Gajewski, K. E. Gilbert, J. McKelvey in *Advances in Molecular Modeling*, vol. 2 (Ed: D. Liotta), JAI Press, Greenwich, CT, USA, **1990**, p. 65.
- [13] C. Lee, W. Yang, R. G. Parr, *Phys. Rev. B* **1998**, 37, 785.
- [14] Y. Nishida, H. Hori, H. Ohru, H. Meguro, *J. Carbohydr. Chem.* **1988**, 7, 239.
- [15] (a) R. Ditchfield, *J. Chem. Phys.* **1972**, 56, 5688; (b) C. Jameson, *Annu. Rev. Phys. Chem.* **1996**, 47, 135.
- [16] L. K. Sanders, E. Oldfield, *J. Phys. Chem. A* **2001**, 105, 8098.
- [17] C. J. Jameson in *Isotopic applications in NMR studies. Isotopes in the Physical and Biomedical Sciences*, Vol. 2 (Eds: E. Buncl, J. R. Jones), Elsevier Science Publishers, Amsterdam, the Netherlands, **1991**, p. 23.
- [18] J. R. Wesener, D. Moskau, H. Günther, *J. Am. Chem. Soc.* **1985**, 107, 7307.
- [19] A. Lycka, P. E. Hansen, *Magn. Reson. Chem.* **1985**, 23, 973.